JOURNAL OF FORENSIC SCIENCES

J Forensic Sci, November 2010, Vol. 55, No. 6
doi: 10.1111/j.1556-4029.2010.01475.x
Available online at: onlinelibrary.wiley.com

PAPER

PHYSICAL ANTHROPOLOGY; ENGINEERING SCIENCES AND PATHOLOGY/BIOLOGY

Timothy G. Baumer,[1] *M.S.; Marcus Nashelsky,*[2] *M.D.; Carolyn V. Hurst,*[3] *B.A.; Nicholas V. Passalacqua,*[3] *M.S.; Todd W. Fenton,*[3] *Ph.D.; and Roger C. Haut,*[1] *Ph.D.*

Characteristics and Prediction of Cranial Crush Injuries in Children*†

ABSTRACT: This study documents four clinical cases of fatal crush injuries to children between 1.5 and 6 years of age with correlations between modeled stress and clinically observed fracture patterns. The clinical case fractures were concentrated in the basicranium, bridged the impact sites, and traversed the middle cranial fossa in the area of the spheno-occipital synchondrosis. The crushing forces from these cases were recreated on a simplified finite element model of a cranium by applying bilateral pressures to corresponding regions. Numerous trials were run to develop a representative pattern of principal stress directions. In all cases, the highest tensile stresses were located on the basicranium and corresponded to the observed fracture path(s). These results suggest that prefailure stress field diagrams may predict fracture propagation paths, although these will not be exact. Also, these analyses indicate that quasi-static bilateral loading of the cranium may lead to predictable fracture of the basicranium.

KEYWORDS: forensic science, pediatric skull, crushing, quasi-static load, basilar fracture, FE modeling

Fracture interpretation is a necessary component of forensic analysis and contributes to the determination of the cause and manner of death. Skeletonized remains, in particular, lack skin and scalp abnormalities that enhance the complete description of a head injury or injuries. Thus, a clear understanding of fracture propagation becomes vital to the forensic professional. Head injuries are often the result of dynamic forces in which a moving object strikes the cranium at a considerable speed or the cranium makes contact with a static object that causes it to rapidly decelerate (1). In cases of crushing injuries, however, a static load is applied relatively slowly to the cranium, initially causing deformation with eventual fracture if pressure continues or increases. In experimental tests on the effects of bilateral crushing forces on cadaver skulls, Russell and Schiller (2) report that avulsion of the petrous portion, fracture through the dorsum sellae, and principal fracture lines running in the direction of the compressive forces were commonly observed features.

There are several case reports of basilar skull damage in the literature involving both crushing and impulse-based loading scenarios, mainly focusing on adult crania. A study of 15 cases of crushing injuries to adult skulls aged 14–63 and experimentally induced crushing fractures on 11 cadaver crania revealed similarities in basilar fracture patterns (2). However, a study by Harvey and Jones (3) claimed that fractures through both petrous bones were not an indicator of impact site. Another study by Yasue (4) then suggested that the overall path of fracture through the basicranium could, in fact, be related to the region of the skull impacted. More recently, a study by Kroman (5) attempted to produce cranial base (hinge) fractures in two unembalmed cadaver adult human crania specimens using a drop tower. High-speed video demonstrated that fractures initiated at the site of impact and propagated through the middle cranial fossa, with some additional minor fractures surrounding the foramen magnum. In this study, the vaults had been removed so it is unclear if the fractures would have terminated at the points of applied forces (fixture and impactor). Kroman further notes a very wide separation of the failing bones during impact, which no doubt would cause very severe soft-tissue damage in the cranial base. This correlates to the high amount of energy and lethality involved in these scenarios.

It is assumed that fractures will generally follow the path of least resistance, but this path may be different between the child and adult cranium. While all of the aforementioned studies focused on adult crania, some recent case reports on quasi-static loading to the crania of children have also presented observations of basilar fractures (1,6). The trend of quasi-static loading producing basilar fractures in both adults and children may suggest that prediction of these fractures is possible.

The finite element (FE) method is a powerful analytical modeling tool that can be used to determine internal stresses and strains within a complex solid. Several studies have shown that maximum principal stress (or strain) directions from a modeled structure correlate well with areas of experimentally or clinically observed bone fractures (7–9). While modeling of fracture propagation generally

[1]Orthopaedic Biomechanics Laboratories, College of Osteopathic Medicine, Michigan State University, East Lansing, MI 48824.
[2]Department of Pathology, University of Iowa Hospitals & Clinics, University of Iowa, Iowa City, IA 52242.
[3]Department of Anthropology, College of Social Sciences, Michigan State University, East Lansing, MI 48824.

*Funded in part by the National Institute of Justice, Office of Justice Programs, United States Department of Justice (2007-DN-BX-K196).
†Presented in part at the 61st Annual Scientific Meeting of the American Academy of Forensic Sciences, February 16-21, 2009, in Denver, CO.

Received 29 May 2009; and in revised form 12 Aug. 2009; accepted 5 Sept. 2009.

involves high computational costs, one theory suggests that there is a close, although not exact, relationship between prefailure stress trajectories and the ultimate path of propagation. In brief, Frank and Lawn (10) proposed that crack growth occurs in such a way as to maximize the energy dissipation per unit length of growth and that the greatest amount of dissipation occurs when the crack plane is perpendicular to the direction of greatest principal tensile stress. In other words, the directions of principal tensile stress developed on a solid may be a reasonable predictor of propagation direction.

In this study, four cases of childhood fatalities from crushing head injuries inflicted by vehicle tires exhibited similar fracture patterns despite differences in age and magnitude of force. This raised the question as to whether certain fracture patterns are indicative of bilateral crushing injuries and if these could be predicted based on the type of loading and the biomechanical properties of the skull.

Materials and Methods

Four cases of fatal crushing head injuries to young children between 1.5 and 6 years of age under known conditions were used as a baseline for applied forces and resulting fracture patterns. In all cases, the head/skull was run over by a vehicle tire, compressing the head/skull between the vehicle tire and the ground. The contact sites and skull fractures were identified and diagramed during autopsy by the investigating forensic pathologist (M.N.). Biomechanical modeling was then conducted in an attempt to recreate and explain the similarities exhibited in the fracture patterns of these cases.

A simplified model of a skull was created in a FE package (Abaqus v.6.3; Hibbitt, Karlsson & Sorensen, Inc., Pawtucket, RI) (Fig. 1). This model consisted of symmetry about the sagittal plane, but not about the coronal or transverse planes. Each major bone of the vault was modeled separately, assumed to have a uniform thickness, and constrained at the suture joints to form the full cranial model. The base of the cranium was modeled as a flat surface with the same thickness as the vault. The primary landmarks in the basal region were modeled: a hole was added to simulate the foramen magnum, dense oblong extrusions lateral to the foramen magnum were generated to represent the petrous portions, and anterior to the foramen magnum the thickness was reduced to represent the region of the spheno-occipital synchondrosis. This model did not utilize specific, age-dependent material properties for the crania and consisted of simplified, although generally accurate, geometry.

The model was subjected to quasi-static pressures corresponding to the specific exterior injury locations for each case. The magnitude of the pressure applied to the cranial model was the same in each case and was scaled down such that the generated stresses would not cause material failure. By restricting the analyses to the elastic region, the exact material properties were not required for this simple analysis. FE analysis was utilized in an effort to reproduce and examine possible relationships between the theoretical prefailure stresses developed on the modeled crania and the fracture patterns observed clinically. Using some basic stress transformation principles at many predefined locations on the skull (FE), the direction and magnitude of tensile and compressive stresses at each location were determined. The full-field map was then filtered to remove all regions of low stress. Areas of tensile (principal) stress were assumed to be the most likely location(s) of potential fracture, and the general trends produced by the model were examined in comparison with the clinical cases. Numerous trials were run within the elastic (nonfailure) range of bone to develop a representative and clearly characterized pattern of principal stress and strain directions.

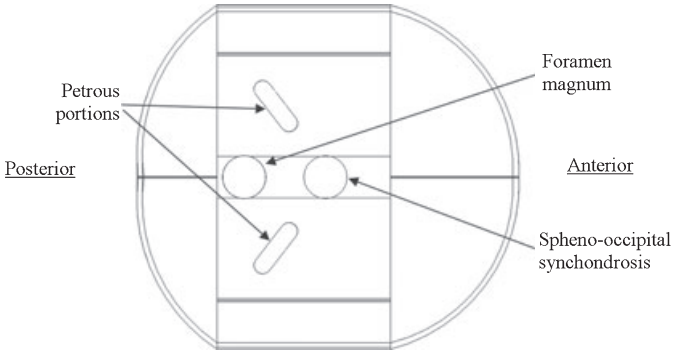

FIG. 1—*Simplified cranial model showing modeled landmarks of the basicranium. View of endocranial surface with vault removed.*

Results

Case 1

A 5-year-old female child was struck by her family's sedan when she fell in an attempt to stop the vehicle after her brother accidentally engaged the transmission. Her head was run over by the right front tire of the car. The autopsy revealed an intact cranial vault with a cranial base fracture that traversed the lateral right anterior cranial fossa, the midline of the middle cranial fossa, and the left lateral aspect of the posterior cranial fossa. This fracture bridged the blunt impact sites on the right anterior and left posterior aspects of the head (Fig. 2).

Case 2

An unhelmeted 6-year-old male was struck by a car while riding his bike. His head was run over by the vehicle's left rear tire.

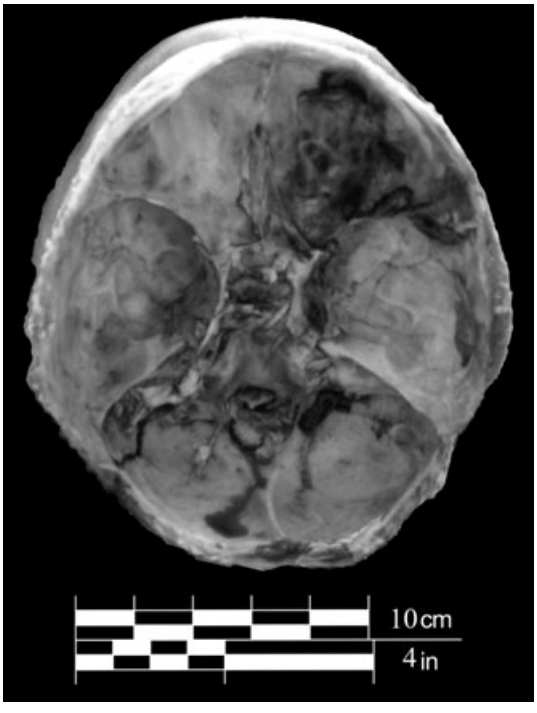

FIG. 2—*Photo taken at autopsy of endocranial base fractures of 5-year-old child from Case 1.*

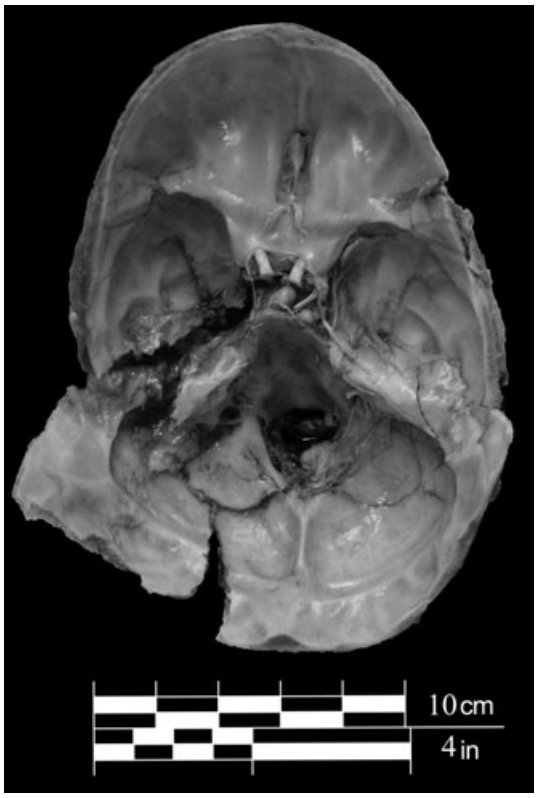

FIG. 3—*Photo taken at autopsy of endocranial base fractures of 6-year-old child from Case 2.*

FIG. 4—*Photo taken at autopsy of endocranial base fractures of 3-year-old child from Case 3.*

Autopsy revealed an intact cranial vault. The cranial base was bisected by a gaping X-shaped fracture centered in the midline of the middle cranial fossa. There were two adjacent arms of the fracture in the right middle cranial fossa. The other two adjacent arms were in the posterior aspect of the left middle cranial fossa and the anterior aspect of the left posterior cranial fossa. This fracture bridged the blunt impact sites on the right anterior and lateral aspects of the head and the left lateral and posterolateral aspects of the head (Fig. 3).

Case 3

A 3-year-old male was run over attempting to run away from a farm grain wagon that had begun to roll. His head was run over by one of the wheels of the wagon. Autopsy revealed gaping linear fractures that traversed the parietal bones and the right and left sides of the frontal bone. One end of each fracture intersected the widely gaping right side of the coronal suture; other ends were continuous with fractures of the cranial base. A dominant cranial base fracture traversed the left petrous bone, the midline of the middle cranial fossa, the anterior aspect of the right middle cranial fossa, and the posterolateral aspect of the right anterior cranial fossa. Additional intersecting fractures were centered in the left middle and posterior cranial fossae (Fig. 4).

Case 4

A 1.5-year-old female was entrapped under a small moving van and her head was run over by the right rear wheel. Autopsy revealed an intact cranial vault but extensive intersecting fractures of the cranial base that predominately traversed the middle and posterior cranial fossae from side to side. A large fracture also bisected the anterior cranial fossae (Fig. 5).

Fracture Pattern Similarities

Each of the cases presented fracture patterns that bridge the impact sites and traversed the middle cranial fossa in the area of the spheno-occipital synchondrosis. Additionally, the damage was concentrated in the basicranium leaving the cranial vault intact in all cases except the 3-year-old boy impacted by the farm grain wagon. Furthermore, general amounts of fracture increased with inferred increase in magnitude of applied force (grain wagon vs. car) or decrease in age.

The four cases presented three contact scenarios with four different fracture configurations, each having commonalities to a single pattern of fracture (described earlier). Specifically, the contact forces in Case 1 were applied primarily to the frontal and occipital bones in a direction between anterior-posterior and lateral (Fig. 6*a*), the contact forces in Cases 2 and 3 were also applied to the frontal and occipital bones but had an additional lateral component (Figs. 7*a* and 8*a*), and the contact forces in Case 4 were applied to the lateral surfaces of the cranial model (Fig. 9*a*).

Modeling of all four cases revealed that the locations of high tensile stress and high tensile strain were the same, and these regions were located on the basicranium. There were some areas of lower tensile stress at the sites of the applied load and in a few areas on the cranial vault, but because of the assumption that failure would occur at locations of high stress, these areas were ignored in this presentation. The maximum tensile stress for all models was similar (standard deviation of ±5%). The tensile

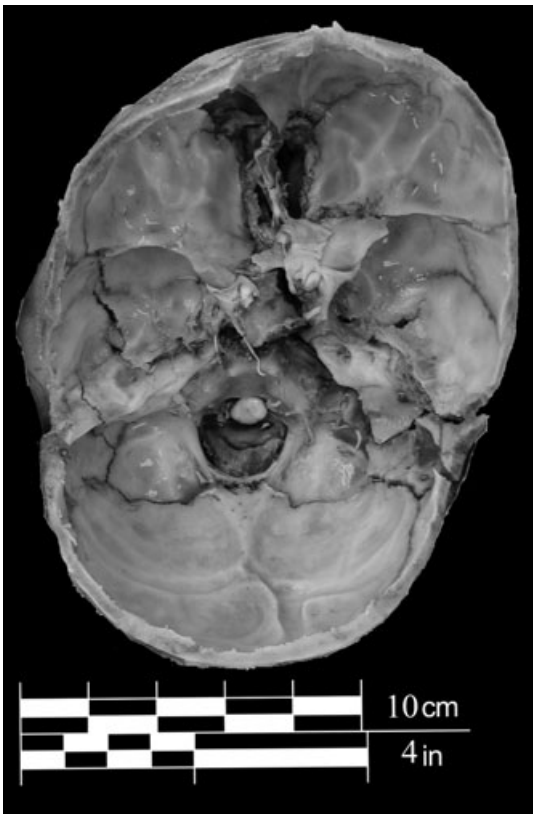

FIG. 5—*Photo taken at autopsy of endocranial base fractures of 1.5-year-old child from Case 4.*

stresses developed on the skull were filtered to display only the highest 20% for correlation to fracture patterns.

Case 1 presented the simplest fracture pattern as a single linear fracture traversing the basicranium from the right greater wing of the sphenoid across the spheno-occipital synchondrosis to the left lateral portion of the occipital, connecting the loading sites (Fig. 6*a*). An overlay of the directions of maximum principal tensile stresses revealed a linear concentration on the right side of the sphenoid and in the area of the spheno-occipital synchondrosis, which correlated well with sections of the observed fracture (Fig. 6*b*).

Cases 2 and 3 presented slightly more complex fracture patterns. In part, the complexity was increased because of the similarities in loading but dissimilarities in fracture (Figs. 7*a* and 8*a*, respectively). A similar fracture in both cases stretched from the right aspect of the sphenoid through the sella turcica and along the superior aspect of the petrous portion of the temporal. The overlay of the directions of maximum principal tensile stresses was identical in both cases because of the similarity of loading patterns. There was correlation between the stress and the fracture for both cases, especially along the line of similar fracture, although each had areas of high stress where fracture did not occur (Figs. 7*b* and 8*b*). Case 4 presented the most complex fracture pattern extending both longitudinally and transversely through the basicranium (Fig. 9*a*). Fractures ran longitudinally across the midline of the anterior cranial fossa and horizontally through the middle and posterior cranial fossa with various areas of comminution. The overlay of the directions of maximum principal tensile stresses revealed an area of complex stress in the same area as the highly comminuted fracture of the right side of the cranial base. Additionally, a more linear pattern of stresses occurred near the fractures on the left side of the skull (Fig. 9*b*).

Discussion

The analyses performed in this study represent a quantitative, theoretical attempt to correlate stress and strain intensities and principal directions to fracture patterns on the skull caused by quasi-static bilateral pressures. A linear, small strain, isotropic, uniform thickness model of a human calvarium was constructed in this study. Analyses of the modeled stresses and the clinically observed fractures suggested that quasi-static bilateral loading of the cranium leads to predictable fracture of the basicranium, although the predictions were not exact. The promising nature of these results suggests that it may be useful to develop a more complex model for a more accurate prediction of fractures on a case-by-case basis.

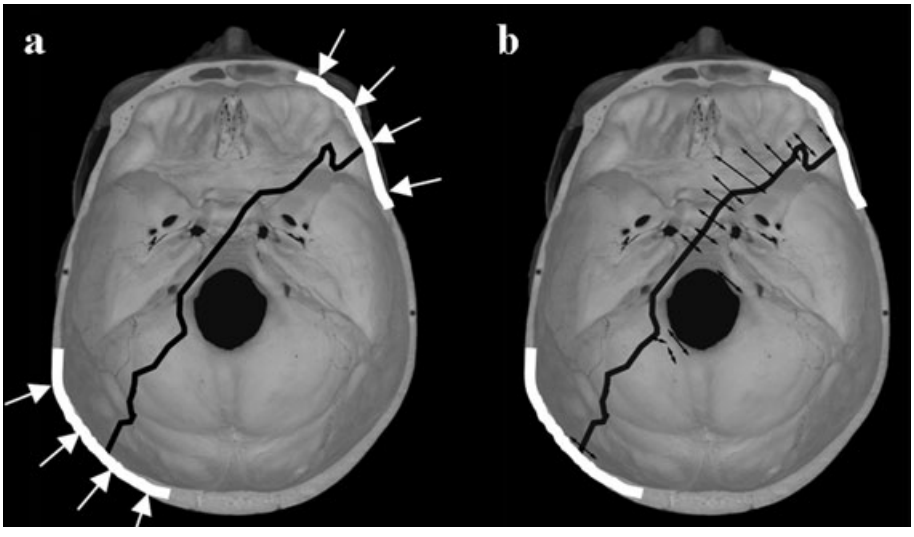

FIG. 6—*(Case 1) Crushing injury to the skull of a 5-year-old. Diagrams of (a) clinically observed fractures and (b) an overlay of the highest 20% of principal tensile stresses produced from a FE model. White cranial margins represent contact of applied forces (ground and tire). The arrows in (b) indicate the directions of tension on the cranium.*

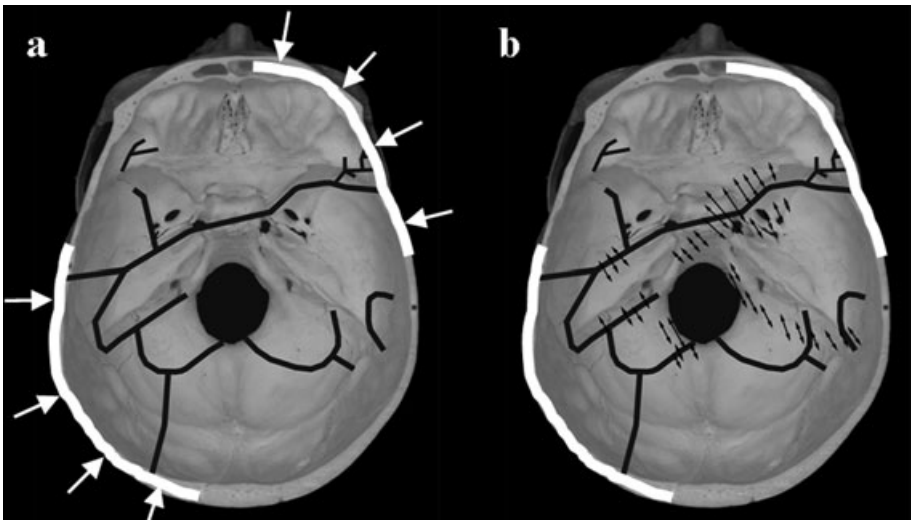

FIG. 7—*(Case 2) Crushing injury to the skull of a 6-year-old. Diagrams of (a) clinically observed fractures and (b) an overlay of the highest 20% of principal tensile stresses produced from a FE model. White cranial margins represent contact of applied forces (ground and tire). The arrows in (b) indicate the directions of tension on the cranium.*

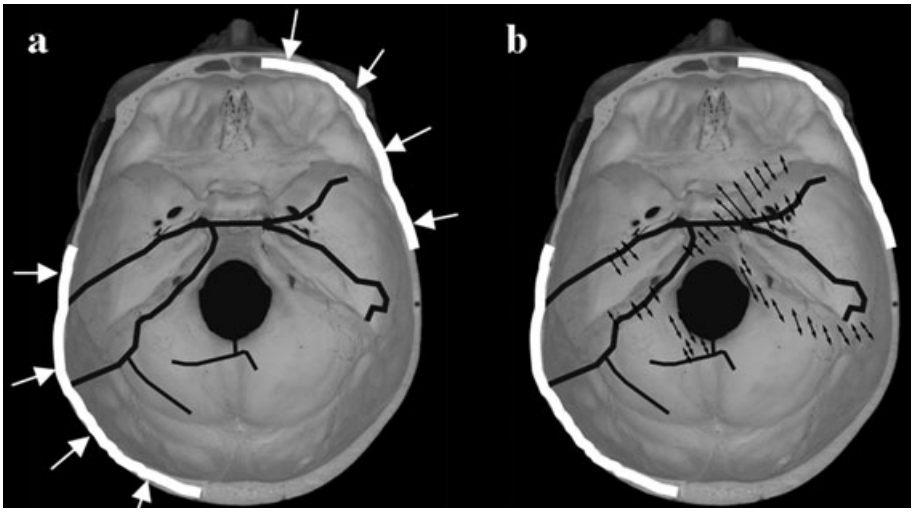

FIG. 8—*(Case 3) Crushing injury to the skull of a 3-year-old. Diagrams of (a) clinically observed fractures and (b) an overlay of the highest 20% of principal tensile stresses produced from a FE model. White cranial margins represent contact of applied forces (ground and tire). The arrows in (b) indicate the directions of tension on the cranium.*

The location of maximum tensile stress would be expected to be the site of fracture initiation, and the location of maximum stress in each of the four models correlated well with the area(s) of fracture in each of the clinical cases. However, Frank and Lawn (10) also suggest that paths of high tensile stress may approximate the path of fracture propagation. In the four cases presented in this study, regions of high tensile stress appeared to follow the path of the fracture extending from the location of maximum stress. Fracture propagation, however, requires increasing levels of stress to overcome the dissipation of energy that occurs with the previous fracturing. These increasing levels of stress may ultimately result in additional fracture sites on the material surface (11). Two or more isolated regions of the skull developed high tensile stresses in Cases 2–4, which may have resulted in multiple sites of fracture initiation with propagation extending from each site. Multiple initiation sites with subsequent propagation joining the sites could explain the complexity of the fractures seen in Cases 2–4, as opposed to the singular region of fracture and stress intensity developed in Case 1. The four cases presented in this study suggest that prefailure stress field diagrams may, in fact, give some insight into the projected fracture propagation paths and, ultimately, fracture patterns developed during quasi-static bilateral loading of the cranium.

The cases and analyses presented in this study supported some general trends for quasi-static bilateral loading scenarios. Autopsy revealed fractures through the middle cranial fossa in the region of the spheno-occipital synchondrosis in all cases. Modeling displayed high tensile stresses through this region in Cases 1–3, with Cases 2 and 3 developing maximum levels of stress at this landmark. However, modeling of Case 4 showed no region of high tensile stress passing through the spheno-occipital synchondrosis. Interestingly, Case 4 involved the youngest child and one of the most massive vehicles (moving van). This result may suggest that the material model should be altered as a function of age, especially for the very young pediatric patient. Autopsies also revealed fractures connecting the loading sites through the basicranium in all four cases. The models showed regions of high tensile stress in this region for

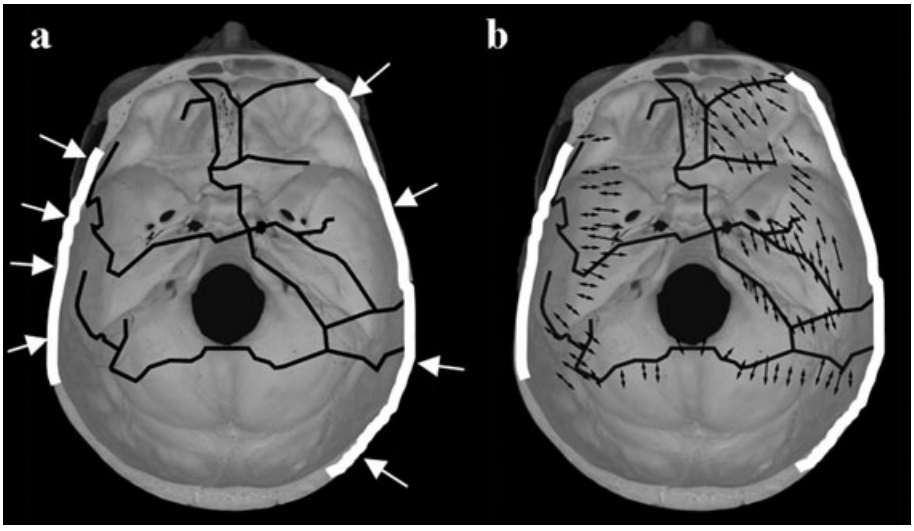

FIG. 9—*(Case 4) Crushing injury to the skull of a 1.5-year-old. Diagrams of (a) clinically observed fractures and (b) an overlay of the highest 20% of principal tensile stresses produced from a FE model. White cranial margins represent contact of applied forces (ground and tire). The arrows in (b) indicate the directions of tension on the cranium.*

Cases 1–3, although the tensile stresses in Case 4 did not seem to follow the same pattern. Intact cranial vaults were also present in three of four cases. The models displayed no significant levels of stress on the vault that would be expected to cause fracture. It is possible that the mass of the vehicle (grain wagon) caused excessive fracture propagation that was not able to be modeled in Case 3. All of the fracture-related observations seen in the current study showed similarities to experimentally developed fractures on adult cadaver skulls (2) suggesting that these patterns of quasi-static loading of the cranium may be somewhat age independent, except for the very young patient, likely as a function of cranial geometry, which would remain essentially the same throughout life.

In summary, a simple model of a cranium subjected to clinically observed bilateral crushing forces was largely able to predict the characteristics of the developed fracture patterns. The results of this study were not meant to propose that the theoretical stresses developed on this simplified cranial model actually predict an arbitrary fracture pattern developed clinically. These results do show that a simplified analysis of tensile stresses developed from some basic information on boundary loads and locations on the cranium could generate patterns of high tensile stress that are consistent with clinical fractures. The four cases, in conjunction with the FE model, suggest that crania subjected to bilateral crushing forces tend to fracture in predictable ways. Further, the regions of high tensile stress that develop between the locations of loading on the pediatric cranium coincide with the locations of tensile fracture.

The predictability of this pediatric cranial fracture pattern has practical application. Medical examiner and coroner death investigations attempt to establish circumstances of injury. In cases of unknown or questionable circumstances, this fracture pattern would suggest a particular mechanism of injury consistent with a heavy wheeled vehicle. The described fracture pattern would be less consistent with other, more common injuries such as those sustained in motor vehicle collisions (ejection or internal tumbling) and in the setting of inflicted blunt trauma. This information may prove relevant in clarifying unexplained perimortem events in cases of crushing injuries to the pediatric cranium, particularly if information from examination of skin and scalp is not possible because of skeletonization.

Acknowledgment

The opinions, findings, and conclusions expressed in this publication are those of the authors and do not necessarily reflect the views of the Department of Justice.

References

1. Duhaime A-C, Eppley M, Margulies S, Heher KL, Bartlett SP. Crush injuries to the head in children. Neurosurgery 1995;37(3):401–7.
2. Russell WR, Schiller F. Crushing injuries to the skull: clinical and experimental observations. J Neurol Neurosurg Psychiatry 1949;12:52–60.
3. Harvey F, Jones A. "Typical" basal skull fracture of both petrous bones: an unreliable indicator of head impact site. J Forensic Sci 1980;25(2):280–6.
4. Yasue M. Clinical and experimental investigation of mediobasal skull fracture. Neurol Med Chir (Tokyo) 1981;21:1041–9.
5. Kroman AM. Fracture biomechanics of the human skeleton [Ph.D. dissertation]. Knoxville (TN): University of Tennessee, 2007.
6. Takeshi M, Okuchi K, Nishiguchi T, Seki T, Watanahe T, Ito S, et al. Clinical analysis of seven patients of crushing head injury. J Trauma 2006;60(6):1245–9.
7. Graham R, Oberlander E, Stewart J, Griffiths D. Validation and use of a finite element model of C-2 for determination of stress and fracture patterns of anterior odontoid loads. J Neurosurg (Spine 1) 2000;93:117–25.
8. Silva M, Keaveny T, Hayes W. Computed tomography-based finite element analysis predicts failure loads and fracture patterns for vertebral sections. J Orthop Res 1998;16:300–8.
9. Doorly M, Gilchrist M. The use of accident reconstruction for the analysis of traumatic brain injury due to head impacts arising from falls. Comput Methods Biomech 2006;9(6):371–7.
10. Frank F, Lawn B. On the theory of Hertzian fracture. Proc R Soc Lond 1967;299(1458):291–306.
11. Paterson M, Wong T. Griffith theory of brittle failure. In: Paterson MS, Wong T-f, editors. Experimental rock deformation—the brittle field. Berlin, Germany: Springer, 2005;45–57.

Additional information and reprint requests:
Roger C. Haut, Ph.D.
Orthopaedic Biomechanics Laboratories
A-407 East Fee Hall
Michigan State University
East Lansing, MI 48824
E-mail: haut@msu.edu